

Conditioned Human Trajectory Prediction using Iterative Attention Blocks

Aleksey Postnikov^{1,2}

Aleksander Gamayunov^{1,2}

Gonzalo Ferrer²

Abstract—Human motion prediction is key to understand social environments, with direct applications in robotics, surveillance, etc. We present a simple yet effective pedestrian trajectory prediction model aimed at pedestrians’ positions prediction in urban-like environments conditioned by the environment: map and surround agents. Our model is a neural-based architecture that can run several layers of attention blocks and transformers in an iterative sequential fashion, allowing to capture the important features in the environment that improve prediction.

We show that without explicit introduction of social masks, dynamical models, social pooling layers, or complicated graph-like structures, it is possible to produce on par results with SoTA models, which makes our approach easily extendable and configurable, depending on the data available. We report results performing similarly with SoTA models on publicly available and extensible-used datasets with uni-modal prediction metrics ADE and FDE.

I. INTRODUCTION

Autonomous mobile robots have recently started walking around us in shops, exhibitions, controlled closed areas around universities and innovative companies. However, human motion is unpredictable by nature, a mind state determining similarly to decision-making and inner motivation processes. Still, recent data-driven approaches have made a great breakthrough on predicting human trajectories [1]–[6] and allow researchers to focus on the most important aspects that might condition such predictions: environment, surrounding agents, past history, or how to interconnect all these components, a task unreachable for past model-based algorithms [7], [8].

Regardless of the limitation on predicting human trajectories, the importance of solving human motion prediction is enormous due to its direct applications. To this end, every year, more methods appear, and they are validated on well accepted benchmarks based on open datasets [9]–[11], competing based on common metrics.

In this paper, we focus on a flexible approach of fusing different data input modalities from observed past pedestrian positions and images from the scene. The flexibility of modern neural-based approaches for the prediction problem allows us to test and verify many different data, such as the perceived environment by map images, the surrounding agents to the ego-agent, etc., and interconnect them in a principled way to obtain the best performance.

¹ The authors are with the Sberbank Robotics Laboratory, Moscow, Russia. {postnikov.a.l, gamayunov.a.r}@sberbank.ru.

²Skolkovo Institute of Science and Technology, Moscow, Russia. g.ferrer@skoltech.ru.

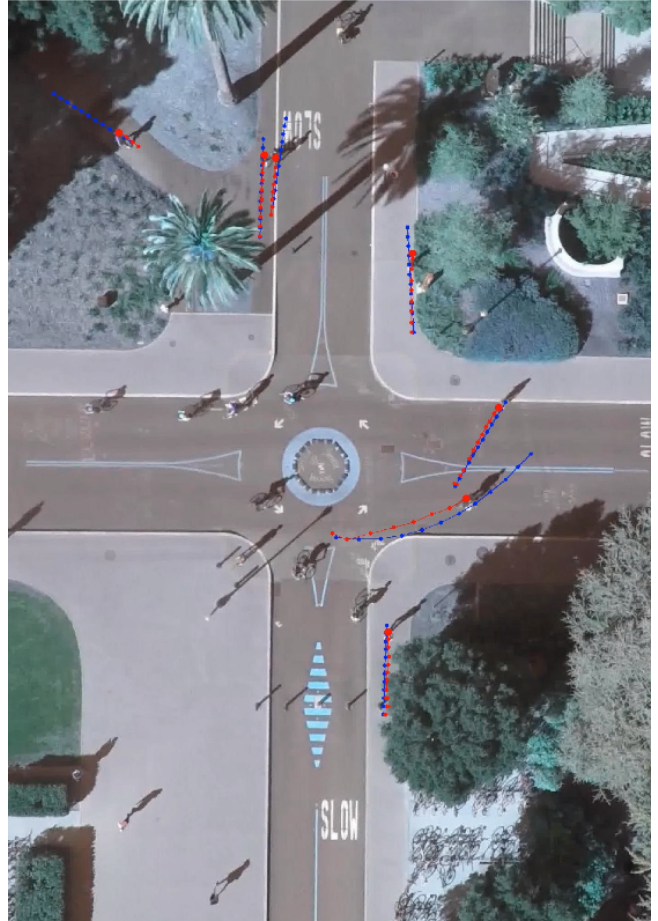


Fig. 1: Visualizations of trajectories predicted by Conditioned Human Trajectory Prediction using Iterative Attention Blocks model (red lines - predictions, blue lines - ground truth trajectories).

To address this task, we propose (i) a perceiver-like [12] encoder block, shown on Figure 3, sequentially mapping data from different modalities with cross-attentions and updating latent vector with transformers and (ii) goal-conditioned iterative approach for generating trajectory predictions, shown at Figure 4.

However, input data preparation is also an essential part of making precise predictions. Therefore, we show preparation the image scene representation before fusing on Figure 2, which keeps useful information about agent direction and start position inside.

This paper’s main contribution is an approach that inter-

leaves a sequence of cross-attention and transformer blocks to capture better the relations between the high dimensional data embeddings from past histories, neighbors positions and RGB bird-eye view images of the environment. The network design is simplified with respect to other approaches, and the results obtained show an on par performance in the ETH [9], UCY [10], and SDD [11] datasets.

II. RELATED WORK

Motion prediction has become a separate task primarily motivated by the effective navigation of the mobile robot in the social environment. Early works were aimed at describing the model of human movement by model-based approach [13], [14]. In some cases of a short prediction horizon or movement on a limited straight sidewalk, the simple linear interpolation or Constant Velocity Model (CVM) [15] can show fairly good accuracy. Still, when there are a lot of pedestrians, it is also necessary to take into account their interaction between each other. This type of interaction can be modeled by Social Force Model (SFM) [13] or more related to the human movement model the Headed Social Force Model (HSFM) [14], which directly take into account such interactions in their model of motion. However, the accuracy of these models strongly depends on how well the destination point is selected, which is used as input data.

In the last years, deep learning approaches have become dominant in the task of Human motion prediction. Modern deep learning frameworks allow optimizing algorithm computation time by utilizing GPU resources. For example, it has been shown [16], [17] how empirical models can be packed into layers-like neural network structures that can use optimized gradient descent to calculate backpropagation loss efficiently.

One of the most popular works that use deep learning approach is Social-LSTM [2] show a simple but effective way of using Recurrent Neural Networks (RNN) [18] variant named Long Short Term Memory (LSTM) [1] blocks for learning general human movement and predict their future trajectories.

There are another deep learning approach based on Generative Adversarial Network (GAN) named SoPhie [6], which leverages path history information with scene context information, using images.

Another deep learning approach utilizes a graph-structured data model. Trajectron [4] and its second version Trajectron++ [5] - multi-agent behavior prediction model that accounts for the dynamics of the agents, produces predictions possibly conditioned on potential future robot trajectories which can effectively use heterogeneous data about the surrounding environment.

PecNet [19] propose estimation of a latent belief distribution modeling the pedestrians' possible endpoints, which are used to predict trajectories. This approach has shown good prediction accuracy, and also it provides additional information about possible trajectories in the outputs, which can be taken into account in trajectory planning step.

The Perceiver [12] propose novel general perception architectures with latent transformers similar to GPT-2 architecture [20], [21], and cross-attention blocks. This work is from a different field of image processing, but despite this, we used some of the ideas from this approach, which we adapted for a human motion prediction field. The main advantage of such an approach is a simplicity and flexibility of architecture while performing on par with the current state of the art [4]–[6].

III. METHOD

A. Problem Formulation

The position of a generic agent $i \in I$ at time t is represented by $u_i^t = (x, y)$, where x, y are the coordinates of agents in the dataset reference system at the instance of time t . The agent's trajectory is defined as $X_i^{1:T} = \{u_i^1, \dots, u_i^T\}$ from timestamp 1 to T .

Every trajectory is split into observed and future: given certain number T_{obs} of observed time step positions, and future states or prediction horizon for the next T_{pred} time steps which is denoted as $p(X_i^{T_{obs}+1:T_{pred}} | X_i^{1:T_{obs}})$.

Following a common practice [1], [2], [4], [15] we use $\Delta t = 0.4s$ between time steps t_i and $T_{obs} = 8; T_{pred} = 12$ steps for scene to be predicted, where overall scene time is $(T_{obs} + T_{pred}) \cdot \Delta t = 8s$. These constraints are used to unambiguously compare an approach and that can be used to solve a problem with another $\Delta t; T_{obs}; T_{pred}$.

The task is to predict the next T_{pred} step positions of a pedestrian with minimum differences to ground truth, based on T_{obs} observed position steps and BEV images for all pedestrians in the scene.

B. Data Preparation

The history of a scene is divided into main agent whose trajectory needs to be predicted X_m , where $m \in I$ and neighbors agents X_n , where $n = \{i | i \in I \setminus m\}$ whose observed trajectories are used as scene context. All coordinates u_i^t are normalized relative to the last known position and direction of the main agent $u_m^{T_{obs}}$ with $T_{o \rightarrow m}$ transformation matrix (1, 2).

Same multi-layer perceptron (MLP) [22] is used to create embedding from agent and neighbors history trajectories:

$$X_m^{emb} = MLP_{pose}(T_{o \rightarrow u_m^{T_{obs}}} \cdot X_m) \quad (1)$$

$$X_n^{emb} = MLP_{pose}(T_{o \rightarrow u_m^{T_{obs}}} \cdot X_n) \quad (2)$$

Where $T_{o \rightarrow m}$ is transformation matrix from original (dataset) coordinate system to centered to last observed position of agent and rotated along the movement of that agent.

Beard Eye View (BEV) RGB images are rotated along to the last known position and direction of the main agent $u_m^{T_{obs}}$ by applying transformation matrix $T_{o \rightarrow u_m^{T_{obs}}}$ and cropped after that as shown on Figure 2 so that last known main agent position always have same image coordinates. The size of cropping square side s depends on the maximum path length for this type of agent, and it is a hyperparameter

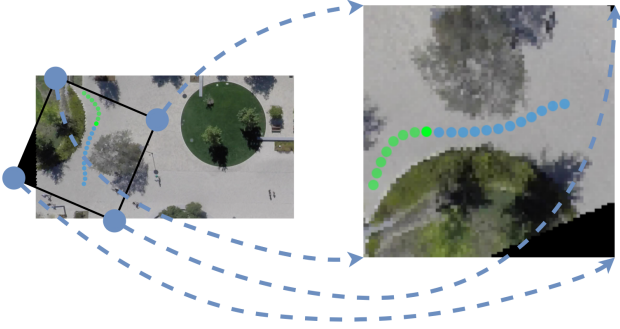


Fig. 2: Image rotation and cropping along the agent position and direction.

of the data preparation module. Agent position centered on image position $[\frac{s}{2}, \frac{s}{4}]$.

We evaluated pretrained Resnet-18 [23], ViT-B/16 [24], and image patching with linear projections [24] to create visual features from cropped and rotated BEV RGB before feeding into encoder.

C. Encoder

We build our architecture from two main components: (i) a cross-attention module that can map latent array and input information of arbitrary shape to a latent array, and (ii) a transformer block that maps a latent array to a latent array. Our model applies the (i) cross-attention module and (ii) the transformer in alternation. This corresponds to projecting the higher-dimensional input information of arbitrary shape through a lower-dimension attention bottleneck before processing it with a deep transformer and then using the resulting representation to query the input again, which allows to effectively fuse different information modalities to the latent array, representing overall scene information.

Model architecture is structured with multiple cross-attention layers, which allow the latent array to iteratively extract information from the input data as it is needed.

The encoder is composed of a stack of N identical blocks. Each block has four sub-blocks, namely three cross-attention modules, that map (i) information about agent history, (ii) neighbors history, (iii) RGB environment map, and (iv) latent transformer to update latent vector. The main processing module of used cross attention and latent transformer is attention, which is permutation-invariant by design, which is inappropriate in case of exploiting temporal nature of observed history information. To preserve temporal information of history positions, we follow the strategy of Fourier feature position encodings [20]. We concatenate 1D positional(temporal) encodings Eq.(3) [20], [25] with agents embedding.

$$\begin{aligned} PE_{(pos, 2i)} &= \sin(pos \cdot e^{\frac{-4 \cdot i}{d_{model}}}) \\ PE_{(pos, 2i+1)} &= \cos(pos \cdot e^{\frac{-4 \cdot i}{d_{model}}}) \end{aligned} \quad (3)$$

Where d_{model} - model embedding dimension, $i \in [0, d_{model})$, specifies model embedding dimension positions, $pos \in [0, T_{obs})$ - specifies temporal positions

Latent transformer block utilizes the GPT-2 [21] architecture, which is itself the decoder of original Transformer [20] architecture. Cross attention is a multi-head attention layer, Eq. (4) that decomposed the attention in multiple heads. The independent attention heads are concatenated and multiplied by a linear layer to match the desired output dimension.

$$MultiHead(Q, K, V) = Concat(h_1, \dots, h_i)W^0 \quad (4)$$

where

$h_i = Attention(QW_i^Q, KW_i^K, VW_i^V)$, $Q = MLP^Q(k)$, $K = MLP^K(k)$, $V = MLP^V(k)$, $W^0 =$ output linear block, i - attention layer, k - input 3-dimensional data.

D. Decoder

We follow the strategy of dividing the trajectory generation problem into two steps: (i) proposing the position of pedestrian goal (goal is pedestrian trajectory point at T_{pred} timestamp), (ii) constructing trajectories conditioned to the proposed goal position.

1) *Goal Decoder*: We decode final endpoint position $u_i^{T_{pred}}$ from encoded latent array, squishing temporal dimension. Multi-Layer Perceptron is used in order to yield our guesses for the final position.

$$u_i^{T_{pred}} = MLP_{goal}(z) \quad (5)$$

where z - latent scene representation vector.

2) *Trajectory Decoder*: The procedure of Trajectories decoding is different for training and inference scenarios. During training, Trajectory predictions are obtained by concatenating encoded 3-dimensional latent array with ground truth goals. During training, ground truth goals are used because it helps to produce cleaner, less noisy signals for downstream prediction networks while still training the overall module end to end [19]. During inference, predicted goals from Goal Decoder are used instead of ground truth goals. Multi-Layer Perceptron is used to decode trajectory.

$$u_i^{T_{obs}+1:T_{pred}} = MLP_{traj}(z, G_{gt}) \quad (6)$$

$$u_i^{T_{obs}+1:T_{pred}} = MLP_{traj}(z, G_{pred}) \quad (7)$$

where G_{gt} is ground truth pedestrian position to be predicted at timestamp T_{pred} , G_{pred} is predicted pedestrian position at timestamp T_{pred}

E. Loss function

The proposed architecture has two separate decoders, namely the Goal decoder and Trajectory decoder, which are trained in an end-to-end manner. We use \mathcal{L}_{FDE} to train Goal Decoder and \mathcal{L}_{ADE} to minimize the error of Trajectory decoder:

$$\begin{aligned} \mathcal{L}_{ADE} &= \frac{\sum_{t=T_{obs}+1}^{T_{pred}} \|u^t - \mu^t\|_2}{T_{pred}} \\ \mathcal{L}_{FDE} &= \|u^{T_{pred}} - \mu^{T_{pred}}\|_2 \\ \mathcal{L}_{model} &= \mathcal{L}_{ADE} + \lambda \cdot \mathcal{L}_{FDE}, \end{aligned} \quad (8)$$

where λ is a regularizer between two losses.

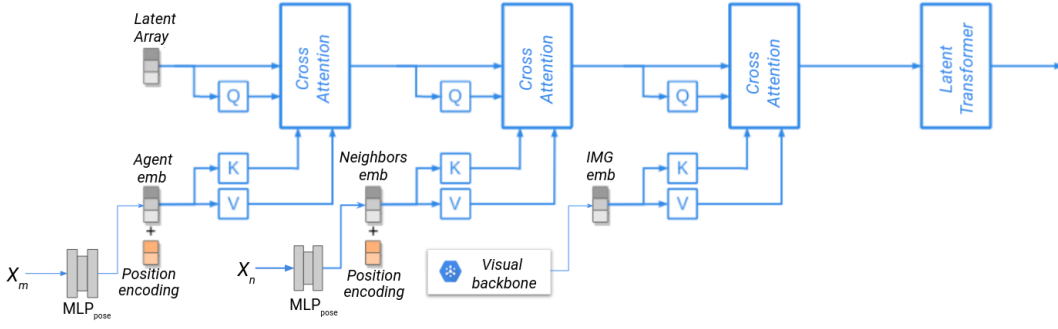


Fig. 3: Encoder block. Different input data modalities embedded and sequentially fed into cross attention blocks.

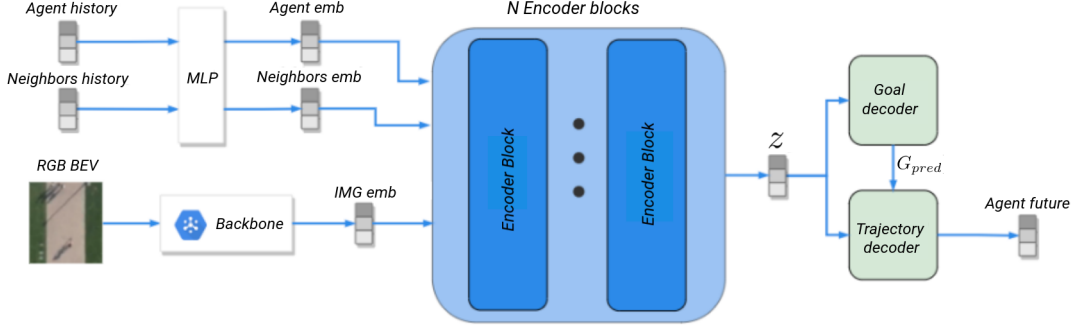


Fig. 4: Proposed architecture. Blue blocks is encoder, iteratively extracting information from the input data, green blocks is decoder part divided on two heads: (i) Goal decoder - to predict the motion target and (ii) Trajectory decoder - to predict the trajectory.

IV. EVALUATION

A. Datasets

The model trained and evaluated on ETH-UCY [9], [10] with Leave-One-Out Cross-Validation (LOOCV) strategy [26] and SDD datasets [11]. The ETH and UCY [9], [10] are publicly available datasets consisted of manual marked pedestrians identifiers and positions on recorded video with 2.5Hz frequency. The videos were recorded from buildings windows and slightly angled, but homography matrices were also attached to datasets for straightening.

The SDD publicly available dataset has identifiers and positions of pedestrians like ETH and UCY, but bigger. It is additionally provides agent class labels such as Pedestrian, Bicyclist, Skateboarder, Cart, Car, Bus, and three flags: “lost” - the annotation is outside of the view screen; “occluded” - the annotation is occluded; “generated” - The annotation was automatically interpolated.

B. Metrics

We use Euclidean distance errors: Average Displacement Error (ADE) (9) and Final Displacement Error (FDE) (10) to evaluate the accuracy. Metrics are formulated as:

$$ADE = \frac{\sum_{j=1}^N \sum_{t=T_{obs}+1}^{T_{pred}} \|u_j^t - \mu_j^t\|_2}{N \cdot T_{pred}} \quad (9)$$

$$FDE = \frac{\sum_{j=1}^N \|u_j^{T_{pred}} - \mu_j^{T_{pred}}\|_2}{N} \quad (10)$$

where N - number of processed pedestrians, u_j^t - ground truth position of j^{th} pedestrian at timestamp t , T_{pred} - prediction horizon, μ - predicted mean position.

C. Compared baselines

Our method is compared against the following baselines: LSTM [1] - LSTM network that process only agent history information by recurrent LSTM layers, S-LSTM [2] - method with LSTM networks that share the information between the state of agents in a scene through the Social pooling layer, S-ATTN [3] - attention-based trajectory prediction model, which uses RNN mixture based approach, modeling both the temporal and spatial dynamics of trajectories in human crowds, Trajectron++ [5] - graph-structured recurrent model, incorporating agent dynamics and heterogeneous data, PecNet [19] model that infers distant trajectory endpoints to assist in long-range multi-modal trajectory prediction, SoPhie [6] - GAN [27] based approach with incorporated social and physical attention mechanisms, Lin - linear pedestrian speed interpolation method that uses the last two observed points, Eq. 11.

$$\begin{aligned} \Delta u_i &= u_i^{T_{obs}} - u_i^{T_{obs}-1} \\ u_i^{t+1} &= u_i^t + \Delta u_i \end{aligned} \quad (11)$$

D. Results

In this section, we compare and discuss our proposed method’s performance against mentioned baselines on the ADE & FDE metrics.

Throughout the following, we report the performance of our approach in multiple configurations. *Our-nomap* represents the base model with only two cross-attention blocks used at every encoder block, namely (i) cross-attention processing embedded agent history positions and (ii) cross-attention processing embedded neighbors positions. *Our-resnet* is the model with all three cross-attention blocks, as shown at figure3, utilising ResNet-18 as a backbone feature extractor. *Our-ViT* is the model with all three cross-attention blocks, with ViT [24] as a backbone feature extractor. *Ours-patch* is the model with all three cross-attention blocks used at every encoder block, as a backbone we split an image into fixed-size patches and linearly embed each of them, similar to ViT [24] patching procedure.

Table I shows results of our proposed methods against baselines and current state-of-the-art methods at ETH-UCY datasets. Our proposed method *Ours-ViT* with ViT [24] feature extractor achieves 18% boost performance at FDE metric comparing to previous state-of-the-art method. Table II shows results of our proposed method against baselines and current state-of-the-art methods at SDD dataset, *Ours-patch* method achieves superior than previous SOTA ADE results.

We show the final displacement error distribution and confidence intervals of our method on Figure 5 for the test data part. Half of all final errors are just in 0.91 meters interval, but we also may observe the long tail of errors resulting from unpredictable human nature. This final error for the 4.8s prediction interval can be too big for some cases, such as a narrow pedestrian road. That error is smaller for shorter prediction intervals, and the robot will adjust the prediction as it approaches a potential intersection with the pedestrian path.

We visualize two-dimensional final error distribution with confidence iso-contours on Figure 5, where each point of that plot is an error, in normalized (according to explained in section III) coordinate system, between ground truth and predicted agent final position from SDD test data part. There are two types of errors that can be distinguished in Figure 5. The first type of error is contour protrusions along the X-axis. The second type of error is contour protrusions on the upper and lower parts of the error distribution. Since we are normalizing the position and orientation of the pedestrian to be predicted at the last observed timestamp in the direction of his movement, the first type of error shows part of the errors when the model correctly predicted the direction of motion but did not correctly predict the value of the person’s movement speed. The second type of error shows scenarios when the model did not correctly predict the direction of movement, which may be associated with unexpected changes in the person’s direction of movement. This type of behavior can be predicted by producing a set of possible trajectories of a person’s movement instead of a single most likely trajectory.

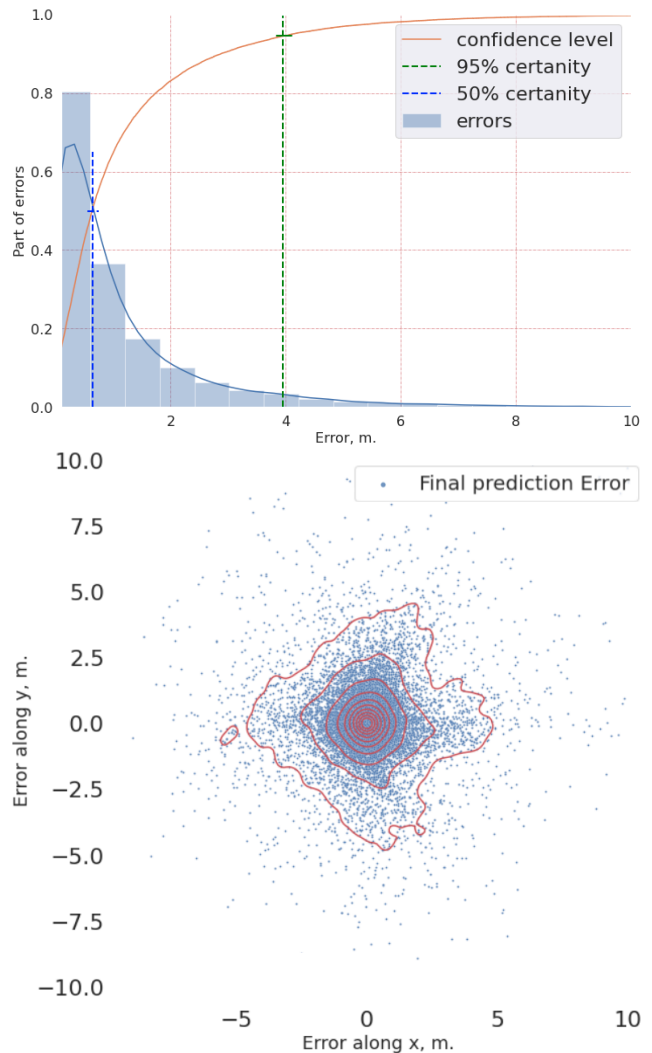


Fig. 5: Distributions of final displacement errors on SDD [11] dataset. Upper: one-dimensional distribution. Lower: two-dimensional distribution.

E. Implementation details

All the sub-networks used in proposed model are Multi-Layered Perceptrons with ReLU non-linearity. Latent array is a learnable array of shape 12×48 , MLP_{pose} is a stacked linear layers with architecture: $2 \rightarrow 8 \rightarrow 32$. MLP_{goal} is a stacked linear layers with architecture: $576 (48 \times 12) \rightarrow 256 \rightarrow 64 \rightarrow 2$. MLP_{traj} is a stacked linear layers with architecture: $50 \rightarrow 256 \rightarrow 64 \rightarrow 24$. Parameters of Multihead Attention layer is next: number of parallel attention heads is 8, embedding dimension is 48 (32 for every pose + 16 of position embedding for every of 12 known positions). The number of sequential encoder blocks used in our model is 4. The entire network is trained end to end with $\mathcal{L}_{model} = \mathcal{L}_{ADE} + \lambda \cdot \mathcal{L}_{FDE}$ loss with $\lambda = 0.5$. Parameters optimization was performed using an ADAM optimizer with a batch size of 32 and initial learning rate of $5e^{-4}$. We decay the learning rate by factor of 0.2 after every 30 epochs. Total number of trained epochs is 65.

TABLE I: Comparison of ADE and FDE results of our method against previously published methods on the ETH [9] and UCY [10] datasets. Both ADE and FDE are reported in meters.

Dataset	LSTM [1]	S-LSTM [2]	S-ATTN [3]	Trajectron++ [5]	SoPhie [6]	Ours-nomap	Ours-ResNet	Ours-ViT	Ours-patch
ETH [9]	1.09/2.41	1.09/2.35	0.39 /3.74	0.71/1.68	0.70/1.43	0.62/ 1.13	0.71/1.35	0.80/1.20	0.64/1.22
Hotel [9]	0.86/1.91	0.79/1.76	0.29/2.64	0.22 /0.46	0.76/1.67	0.29/0.42	0.40/0.57	0.26/ 0.37	0.35/0.65
Univ [10]	0.61/1.31	0.67/1.40	0.33 /3.92	0.41/1.07	0.54/1.24	0.62/0.96	0.62/1.03	0.66/ 0.92	0.70/1.12
Zara 1 [10]	0.41/0.88	0.47/1.00	0.20 / 0.52	0.30/0.77	0.30/0.63	0.61/1.24	0.61/0.70	0.53/0.73	0.53/1.13
Zara 2 [10]	0.52/1.11	0.56/1.17	0.30/2.13	0.23 /0.59	0.38/0.78	0.41/0.70	0.44/0.58	0.39/ 0.56	0.40/0.82
Mean:	0.70/1.52	0.72/1.54	0.30 /2.59	0.37/0.95	0.54/1.15	0.50/0.90	0.55/0.84	0.52/ 0.75	0.53/0.98

TABLE II: Comparison of ADE and FDE results of our method against previously published methods on the SDD [11] dataset. Both ADE and FDE are reported in pixels. *measured with deterministic setup (k=1)

	PecNet [19]	S-LSTM [2]	Lin	SoPhie [6]	DESIRE	Ours-ResNet	Ours-ViT	Ours-patch
ADE:	37.70*	31.19	19.70	16.27	19.25	15.97	15.57	15.54
FDE:	88.17*	56.97	39.60	29.38	34.05	31.35	30.35	30.92

V. CONCLUSION

In this paper, we have proposed a trajectory prediction algorithm conditioned by multiple sources of input data. Our approach first creates the embeddings of data from map images using a pre-trained backbone network and the past history of agents from a multilayer perceptron. Our main contribution is on how to combine the high dimensional embeddings from data into an approach that uses cross-attention and transformers iteratively, allowing to effectively capture the complex relations between the ego-agent prediction and the environment.

Our proposed method results in simplified network architecture, more flexible for further configurations or modifications while its performance is similar to other SoTA approaches, being best at some sequences.

REFERENCES

- [1] Hochreiter, Sepp and Schmidhuber, Jürgen “Long short-term memory” *Neural computation*, vol. 9, no. 8, pp 1735-1780, 1997.
- [2] Alahi A. et al. “Social lstm: Human trajectory prediction in crowded spaces” *Conference on Computer Vision and Pattern Recognition (CVPR)*. – *IEEE Computer Society*, pp 961-971, 2016.
- [3] Vemula, Anirudh and Muelling, Katharina and Oh, Jean “Social attention: Modeling attention in human crowds” in *IEEE international Conference on Robotics and Automation (ICRA)*, pp 4601-4607, 2018.
- [4] Ivanovic, B., Pavone, M. “The trajectron: Probabilistic multi-agent trajectory modeling with dynamic spatiotemporal graphs” In: *Proceedings of the IEEE International Conference on Computer Vision*, pp. 2375–2384, 2019.
- [5] Salzmann, Tim and Ivanovic, Boris and Chakravarty, Punarjay and Pavone, Marco “Trajectron++: Dynamically-feasible trajectory forecasting with heterogeneous data” *arXiv preprint arXiv:2001.03093*, 2020.
- [6] Sadeghian, Amir and Kosaraju, Vineet and Sadeghian, Ali and Hirose, Noriaki and Rezatofghi, Hamid and Savarese, Silvio “Sophie: An attentive gan for predicting paths compliant to social and physical constraints” *Proceedings of the IEEE/CVF Conference on Computer Vision and Pattern Recognition*, pp.1349-1358, 2019.
- [7] Ferrer, Gonzalo et al. “Robot social-aware navigation framework to accompany people walking side-by-side” *Autonomous Robots*, 41(4): 775–793, 2017
- [8] Ferrer, G. and Sanfeliu, A. “Behavior Estimation for a Complete Framework for Human Motion Prediction in Crowded Environments” in *IEEE international Conference on Robotics and Automation (ICRA)*, pp 5940-5945, 2014.
- [9] Pellegrini S. et al. “You’ll never walk alone: Modeling social behavior for multi-target tracking” *2009 IEEE 12th International Conference on Computer Vision*, pp 261-268, 2009
- [10] Lerner, Alon and Chrysanthou, Yiorgos and Lischinski, Dani “Crowds by example” *Computer graphics forum*, vol. 26, no. 3, pp 655-664, 2007
- [11] Robicquet A. et al. “Learning social etiquette: Human trajectory understanding in crowded scenes” *European conference on computer vision*, pp 549-565, 2016
- [12] Jaegle A. et al. “Perceiver: General perception with iterative attention” *arXiv preprint arXiv:2103.03206*, 2021
- [13] Helbing, D., & Molnar, P. “Social force model for pedestrian dynamics” *Physical review E*, vol. 51, no. 5, pp 4282, 1995.
- [14] Farina F. et al. “Walking Ahead: The Headed Social Force Model” *PLoS one*, vol. 12, no. 1, pp e0169734, 2017.
- [15] Schöller C. et al. “What the constant velocity model can teach us about pedestrian motion prediction” *IEEE Robotics and Automation Letters*, vol. 5, no. 2, pp 1696-1703, 2020.
- [16] Postnikov, A., Gamayunov, A., Ferrer, G. “HSFM- Σ nn: Combining a Feedforward Motion Prediction Network and Covariance Prediction” *arXiv preprint arXiv:2009.04299*, 2020.
- [17] Mehta, D., Ferrer, G., Olson, E. “Backprop-MPDM: Faster risk-aware policy evaluation through efficient gradient optimization” *2018 IEEE International Conference on Robotics and Automation (ICRA)*, pp 1740-1746, 2018.
- [18] Rumelhart, David E and Hinton, Geoffrey E and Williams, Ronald Jürgen “Learning representations by back-propagating errors” *nature*, vol. 323, no. 6088, pp 533-536, 1986.
- [19] Mangalam K. et al. “It is not the journey but the destination: Endpoint conditioned trajectory prediction” *European Conference on Computer Vision*, pp. 759–776, 2020.
- [20] Vaswani A. et al. “Attention is all you need” *arXiv preprint arXiv:1706.03762*, 2017
- [21] Radford A. et al. “Language models are unsupervised multitask learners” *OpenAI blog*, vol. 1, no. 8, pp 9, 2019
- [22] Ramchoun H. et al. “Multilayer Perceptron: Architecture Optimization and Training.” *IJIMAI*, vol. 4, no. 1, pp 26-30, 2016
- [23] He K. et al. “Deep residual learning for image recognition” *Proceedings of the IEEE conference on computer vision and pattern recognition*, pp 770-778, 2016
- [24] Dosovitskiy, Alexey, et al. “An image is worth 16x16 words: Transformers for image recognition at scale.” *arXiv preprint arXiv:2010.11929*, 2020
- [25] Wang, Zelun and Liu, Jyh-Charn “Translating math formula images to LaTeX sequences using deep neural networks with sequence-level training” *International Journal on Document Analysis and Recognition (IJ DAR)*, pp 1-13, 2020
- [26] Molinaro, Annette M and Simon, Richard and Pfeiffer, Ruth M “Prediction error estimation: a comparison of resampling methods” *Bioinformatics*, vol. 21, no. 15, pp 3301-3307, 2005
- [27] Goodfellow I. et al. “Generative adversarial nets in advances in neural information processing systems (NIPS)” *Springer New York*, 2014.